Local Control Strategies for Groups of Mobile Autonomous Agents

LIN Zhiyun
zhiyun.lin@utoronto.ca

Mireille Broucke
broucke@control.utoronto.ca
416-978-0803
fax: 416-978-0804

Bruce Francis*
bruce.francis@utoronto.ca
416-978-6343
fax: 416-978-0804

Electrical and Computer Engineering
University of Toronto
Toronto, M5S 3G4
Canada

Keywords: mobile autonomous agents, distributed control

Abstract

The problem is studied of achieving a specified formation among a group of mobile autonomous agents. The focus is on three alignment strategies. In the first, agent 1 should pursue agent 2, agent 2 should pursue agent 3, etc. It is well known that under this strategy all agents converge to a point. We also study whether collisions occur, showing that if the agents initially are arranged in a counterclockwise or clockwise star formation, then they are always so arranged and no collisions occur. A modified strategy is also studied, where agent i pursues a virtual displacement of agent $i+1$, and achievable formations are characterized.

In the second alignment strategy, each agent can see only its neighbor agents, typically those within a given radius. We develop a strategy for each agent based on such a sensor. The situation is more complicated than the first, because agents may go in and out of another agent's sensor range, so the model is time-varying. Our strategy is proved to result in convergence of all agents to a point.

In the third alignment strategy, each agent senses a subgroup of agents and pursues the centroid of the subgroup. We represent the sensing relationship among a group of mobile autonomous agents by a directed graph where the vertices represent the agents. Convergence is proved for whatever field of view, despite the absence of centralized coordination and despite the fact that the subgroup of agents sensed by each agent changes over time as the system evolves. Furthermore, a more general control strategy is concluded to achieve the same result.

*Corresponding author

1 Introduction

In 1987 Craig Reynolds [4] introduced an elaborate model and wrote a program called *boids* [5] that simulates a flock of birds in flight; they fly as a flock, with a common average heading, and they avoid colliding with each other. Each bird has a local control strategy—there's no leader broadcasting instructions—yet a desirable overall group behavior is achieved. The local strategy of each bird has three components: *separation*, steer to avoid crowding; *alignment*, steer towards the average heading of neighbors; *cohesion*, steer towards the average position of neighbors. Recently, Jadbabaie et al. [3] formulated a simple mathematical 2-dimensional version of Reynolds' setup and studied one of the steering strategies. They proved that the alignment strategy leads, under a certain assumption (the graph modeling who are neighbors of whom always is connected, or at least periodically connected), to the result that all the agents' headings converge to a common heading.

Besides being of interest in biology (where it is apparently not well understood how birds flock or fish school), Reynolds' ideas have relevance in the subject of multiple vehicle formations, e.g., [9], [12], [17]. Generally, the objective is for a group of mobile agents (robot rovers, unmanned air vehicles, or unmanned underwater vehicles) either to achieve a formation, or to move while maintaining a formation, or to reconfigure from one formation to another.

The study of the problem of achieving global behavior in a group of robots using only local control strategies can be traced back 125 years. As mentioned in [2], Edouard Lucas (1877) had proposed the following problem: "Three dogs are placed at the three vertices of an equilateral triangle; they run one after the other, what is the curve described by each of them?" and Henri Brocard (1880) gave the solution: "Let us suppose that the three dogs start simultaneously and with the same speed, the pursuit curve for each dog is a logarithmic spiral which is equiangular, and three dogs meet at a point in the center of the triangle known as a Brocard point."

More recently, several researchers began investigating issues in distributed algorithms for multi-agent systems. In [12], a group of simulated robots form approximations to circles and simple polygons, using the scenario that each robot orients itself to, e.g., the furthest and nearest robot. In [16], a similar setup is presented, but the collision avoidance and the group motion, e.g., a matrix formation performing a right turn, are also considered. And in [7], [19], [20], distributed point convergence algorithms are discussed, where a large set of robots represented as points in the plane congregate at a single position. Moving synchronously in discrete time steps, robots iteratively observe neighbors within some visibility range, and follow simple rules to update their positions. Also, research papers focusing on the detailed mathematical analysis of emergent behavior are beginning to appear. One example is the use of nearest-neighbor tracking strategies, where simple navigation rules are used locally to generate desired global formations. For example, in [14] and [15], Wang proposed a scheme where agents are instructed to track the motions of their nearest neighbor, while one agent is provided with a reference trajectory and is designated to be the group leader. In [10], the key idea was that each robot keeps a single friend at a desired angle to have n mobile robots establish and maintain some predetermined geometric shape. Paper [17] addresses distributed structural stabilization of a formation of multiple vehicles using structural potential functions obtained naturally from the formation graphs of the vehicles. In [13], artificial potential functions are used for coordination of multiple vehicles.

In this paper we study the suitability of three alignment strategies. In the first, we suppose the agents have been numbered and marked, from 1 to n. Agent 1 can always see agent 2, agent 2 can always see agent 3, and so on, and finally agent n can always see agent 1. Thus the agents need be outfitted only with on-board local sensors, such as cameras. The strategy is that agent 1 should pursue agent 2, agent 2 should pursue agent 3, etc. It is well known that under this strategy all agents converge to a point. We give a simple proof of this fact. We also study whether collisions occur. We show that if the agents initially are arranged in a counterclockwise star formation or a clockwise star formation, then they are always so arranged, and therefore there is no collision. Of course, all agents being at a point is very specialized as a desirable configuration. So we study a modified strategy, where agent i pursues a virtual displacement of agent $i+1$ (and agent n pursue a virtual displacement of agent 1). We study the achievable formations in this case.

In the second alignment strategy, each agent can see only its neighbor agents, typically those within a given radius. We develop a strategy for each agent based on such a sensor. The situation is more complicated than the first, of course, because agents may go in and out of another agent's sensor range, so the model is time-varying and could be modeled as a hybrid system. Our strategy is proved to result in convergence of all agents to a point.

In the third alignment strategy, each agent senses a subgroup of agents and pursues the centroid of the subgroup. We represent the sensing relationship among a group of mobile autonomous agents by a directed graph where the vertices represent the agents. Convergence to a point is proved for whatever field of view, despite the absence of centralized coordination and despite the fact that the subgroup of agents sensed by each agent changes over time as the system evolves. Furthermore, a more general control strategy is concluded to achieve the same result. Finally, the feasibility of implementing our control strategies using local sensors is discussed.

Our setup is extremely simple: An agent is a point in the complex plane with no kinematic constraints of motion. In future work the agents will be wheeled vehicles with non-holonomic kinematic constraints.

2 A Strategy Based on Sequential Pursuit

Consider n ordered and numbered points, $z_1, \ldots, z_n$, in the complex plane. Each represents a freely mobile agent. We consider the local strategy where each agent pursues the next one in the order. Thus, for example, agent 1 pursues agent 2, so that the kinematic equation is

$$\dot{z}_1 = z_2 - z_1. \tag{1}$$

Agent n pursues agent 1. In this way the overall model is

$$\dot{z}_i = z_{i+1} - z_i, \quad i = 1, \ldots, n-1,$$

$$\dot{z}_n = z_1 - z_n,$$

or, in vector form,

$$\dot{z} = Az, \tag{2}$$

where A has the form $A = P - I$ and P is the permutation matrix obtained by taking I and putting its first row at the bottom:

$$P = \begin{bmatrix} 0 & 1 & 0 & \dots & 0 \\ 0 & 0 & 1 & \dots & 0 \\ \vdots & \vdots & \vdots & \vdots & \vdots \\ 1 & 0 & 0 & \dots & 0 \end{bmatrix}.$$

It is interesting to observe that system (2) can be written as the closed-loop system for a suitably defined decentralized feedback control law:

$$\dot{z}(t) = u(t),$$

with the velocity control input

$$u(t) = -e(t), \tag{3}$$

where $e(t)$ is the error vector

$$e(t) := (I - P)z(t).$$

Notice in (1) that the velocity of z_1 is not constant in magnitude: The point slows down as z_1 approaches z_2. This is to keep the system linear. The constant-speed model would have been

$$\dot{z}_1 = \frac{z_2 - z_1}{|z_2 - z_1|}.$$

We don't study this case.

Theorem 1 *Concerning system (2), for all initial locations of the agents, the centroid of the points $z_1(t), \dots, z_n(t)$ is stationary and every $z_i(t)$, $i = 1, 2, \dots, n$ converges to this centroid.*

Proof The characteristic polynomial of P is $s^n - 1$. So the eigenvalues of P are the n^{th} roots of unity, and therefore the eigenvalues of A are these roots of unity shifted left a distance of 1. That is, A has an eigenvalue at the origin and $n - 1$ distinct eigenvalues strictly in the left half-plane.

An eigenvector, v, for the zero eigenvalue satisfies $Av = 0$, i.e., $Pv = v$. Thus all the components of v are equal. Take them all to be 1. The corresponding eigenspace, $\mathcal{E}_0$, is one-dimensional.

Let $\mathcal{E}_1$ denote the sum of all the other eigenspaces. It is claimed that $\mathcal{E}_0$ and $\mathcal{E}_1$ are orthogonal. To see this, let λ be a nonzero eigenvalue and w a corresponding eigenvector. Then

$$Pw = w + \lambda w.$$

Pre-multiply by v^T and use the fact that $v^T P = v^T$ since v is all 1's:

$$v^T w = v^T w + \lambda v^T w.$$

Thus $v^T w = 0$.

Now consider the motion of $\dot{z} = Az$. The initial state can be factored as

$$z(0) = av + w(0), \tag{4}$$

where a is a constant, so $av \in \mathcal{E}_0$, and $w(0) \in \mathcal{E}_1$. Pre-multiply (4) by v^T and use orthogonality of $\mathcal{E}_0$ and $\mathcal{E}_1$ to get that

$$v^T z(0) = a \times n,$$

that is, $a = (z_1(0) + \cdots + z_n(0))/n$, the centroid of the initial points. The trajectory looks like

$$z(t) = av + w(t), \quad w(t) \in \mathcal{E}_1.$$

Again, pre-multiplying by v^T, we get that $v^T z(t)$ is a constant. Thus, the centroid of the points $z_1(t), \ldots, z_n(t)$ is stationary.

Finally, since $w(t) \to 0$, we have $z(t) \to av$, so that each $z_i(t)$ converges to a. ■

Figure 1 demonstrates a simulation for six mobile autonomous agents using the local control strategy based on sequential pursuit. Six agents are ordered and numbered clockwise. As another example, the simulation result for converging to a single point of ten mobile autonomous agents is shown in Figure 2. Here ten agents are ordered and numbered randomly. From Figure 2, it can be seen that the trajectories of these autonomous agents may overlap.

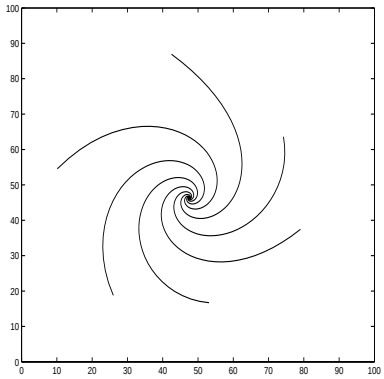

Figure 1: Trajectories of six agents converging to a single point.

Now we consider a modified strategy where each agent pursues a displacement of the next agent:

$$\dot{z}_i = (z_{i+1} + c_i) - z_i, \quad i = 1, \ldots, n-1,$$

$$\dot{z}_n = (z_1 + c_n) - z_n.$$

The vector form is

$$\dot{z} = Az + c. \tag{5}$$

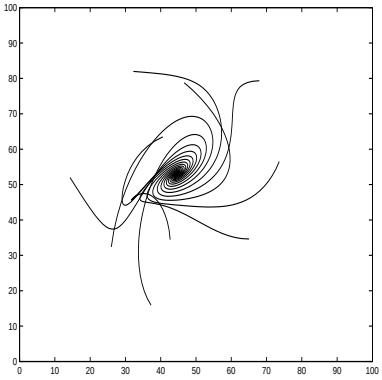

Figure 2: Trajectories of ten agents converging to a single point.

Pre-multiply by v^T:

$$v^T \dot{z} = v^T c.$$

Thus if $v^T c \neq 0$, that is, if the centroid of the points $c_1, \ldots, c_n$ is not at the origin, then the centroid of the agents moves off to infinity. To avoid this, we must assume that $v^T c = 0$. Then $c \in \mathcal{E}_1$, the stable eigenspace, and there is a unique $d \in \mathcal{E}_1$ such that $Ad + c = 0$.

Theorem 2 *Concerning system (5), assume the centroid of the points $c_1, \ldots, c_n$ is at the origin. Then for any initial positions of the agents, the centroid of the points $z_1(t), \ldots, z_n(t)$ is stationary and every $z_i(t)$ converges to this centroid displaced by d_i.*

Proof The equation

$$\dot{z} = Az + c$$

can be written as

$$\frac{d}{dt}[z(t) - d] = A[z(t) - d + d] + c = A[z(t) - d].$$

¿From Theorem 1, the centroid of the points $z_1(t) - d_1, \ldots, z_n(t) - d_n$ is stationary and every $z_i(t) - d_i$ converges to this centroid. But the centroid of the points $z_1(t) - d_1, \ldots, z_n(t) - d_n$ equals the centroid of the points $z_1(t), \ldots, z_n(t)$. ■

We simulate the modified control strategy where each agent pursues a displacement of the next agent for six mobile autonomous agents as shown in Figure 3. The initial locations of the six agents are randomly produced and the displacement vector is

$$c = \left[\begin{array}{cccccc} -5 + j5\sqrt{3}, & -5 + j5\sqrt{3}, & 10, & 10, & -5 - j5\sqrt{3}, & -5 - j5\sqrt{3} \end{array} \right]^T.$$

The simulation result shows that the group of agents achieves an equilateral triangle formation. Also, Figure 4 shows a simulation for six mobile autonomous agents to achieve a line formation using the same control strategy where the displacement vector is

$$c = \left[\begin{array}{cccccc} 10, & 10, & 10, & 10, & 10, & -50 \end{array} \right]^T.$$

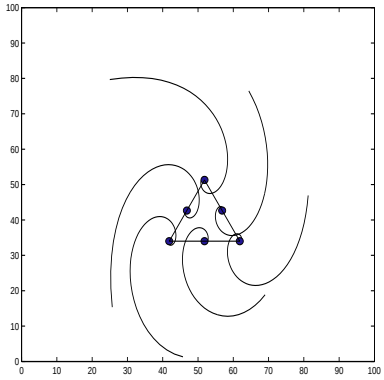

Figure 3: Achieving an equilateral triangle formation for six mobile agents.

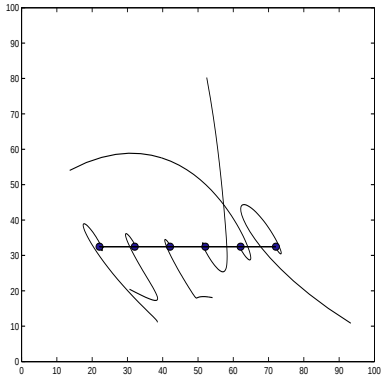

Figure 4: Achieving a line formation for six mobile agents.

Now we turn to the issue of collision avoidance. A *collision* occurs if $z_i(t) = z_j(t)$ for some t and $i \neq j$. Of course the setup is very idealized, as the agents are modeled as points and collisions must therefore be very rare events indeed. Our study is actually more general and concerns how the arrangement of agents evolves.

We begin with a tool for studying angles. Let $\overrightarrow{z_2 z_1}$ denote the directed line segment from a point z_2 to another point z_1.

Lemma 1 *Let z_1, z_2, z_3 be three points in the complex plane, as shown in Figure 5. Let α denote the counterclockwise angle from line $\overrightarrow{z_2 z_1}$ to line $\overrightarrow{z_2 z_3}$, $r_1 = |z_1 - z_2|$ and $r_3 = |z_3 - z_2|$. Define $F = \Im\{\overline{(z_1 - z_2)}(z_3 - z_2)\}$. Then*

(a) *$0 < \alpha < \pi$, $r_1 > 0$, and $r_3 > 0$ iff $F > 0$,*

(b) *$\pi < \alpha < 2\pi$, $r_1 > 0$, and $r_3 > 0$ iff $F < 0$,*

(c) *the points are collinear iff $F = 0$.*

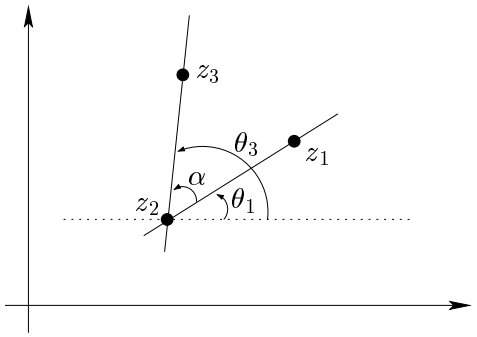

Figure 5: Illustration for points z_1, z_2, z_3 and angles $\alpha, \theta_1, \theta_3$.

Proof We introduce polar form:

$$z_1 - z_2 = r_1 \mathrm{e}^{j\theta_1}, \quad z_3 - z_2 = r_3 \mathrm{e}^{j\theta_3},$$

where θ_1, θ_3 are the angles shown in Figure 5. Then

$$F = \Im\{\overline{(z_1 - z_2)}(z_3 - z_2)\} = \Im\{r_1 \mathrm{e}^{-j\theta_1} r_3 \mathrm{e}^{j\theta_3}\} = \Im\{r_1 r_3 \mathrm{e}^{j\alpha}\} = r_1 r_3 \sin(\alpha).$$

Thus, $r_1 > 0$, $r_3 > 0$, and $0 < \alpha < \pi$ iff $F > 0$; and $r_1 > 0$, $r_3 > 0$ and $\pi < \alpha < 2\pi$ iff $F < 0$. Also, $F = 0$ iff $\alpha = 0$, $\alpha = \pi$, $r_1 = 0$, or $r_3 = 0$, i.e., the points are collinear. ■

Now we return to the system of n agents. Consider n distinct points $z_1, \ldots, z_n$, not all collinear. Let z_0 be their centroid and r_i be the distance between z_i and the centroid. Let α_i denote the counterclockwise angle from line $\overrightarrow{z_0 z_i}$ to line $\overrightarrow{z_0 z_{i+1}}$ for $i = 1, \ldots, n-1$ and α_n denote the counterclockwise angle from line $\overrightarrow{z_0 z_n}$ to line $\overrightarrow{z_0 z_1}$. See Figure 6.

Definition 1 *The n points are said to be arranged in a* counterclockwise star formation *if $r_i > 0$ and $\alpha_i > 0$ for all $i = 1, \ldots, n$ and $\sum_{i=1}^n \alpha_i = 2\pi$. They are said to be arranged in a* clockwise star formation *if $r_i > 0$ and $\alpha_i < 0$ for all $i = 1, \ldots, n$ and $\sum_{i=1}^n \alpha_i = -2\pi$.*

In what follows, we consider only counterclockwise star formations, since clockwise star formations require an analogous treatment. Also, the case $n = 2$ is trivial, so is omitted. First we require the following.

Lemma 2 *Suppose that n distinct points $z_1, \ldots, z_n$ with $n > 2$ form a counterclockwise star formation. Then $\alpha_i < \pi$.*

Proof Suppose by way of contradiction and by renumbering the points, if necessary, that $\alpha_1 \geq \pi$. Now we fix a coordinate system centered at z_0 with the positive real axis given by the ray from z_0 passing through z_1. Then we have $\Im\{z_1\} = 0$, $\Im\{z_2\} \leq 0$ and $\Im\{z_k\} < 0$ for $k = 3, \ldots, n$. Hence, $\Im\{z_0\} = \sum_{i=1}^n \frac{\Im\{z_i\}}{n} < 0$, a contradiction. ■

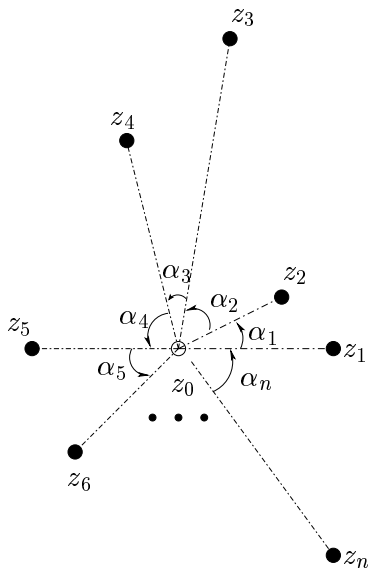

Figure 6: A counterclockwise star formation.

Lemma 3 *If n points $z_1, \ldots, z_n$ are all collinear at some time t_1, then they are collinear for all $t < t_1$ and $t > t_1$.*

Proof Suppose the n (not necessarily distinct) points are all collinear at $t = t_1$. We reorient the coordinate system so that they lie on the real axis $\mathbb{R}$. Considering the system equation (2), if $z_i \in \mathbb{R}$, $i = 1, \ldots, n$, then $\dot{z}_i \in \mathbb{R}$, $\forall i$. This means $\mathbb{R}^n$ is an invariant subspace of system (2). Hence, $z_i(t) \in \mathbb{R}$ for all time, implying the points are collinear for all t. ■

Theorem 3 *Suppose that n distinct points, with $n > 2$, initially are arranged in a counterclockwise star formation. Then the points remain in a counterclockwise star formation; in particular, they never collide.*

Proof Consider the functions

$$\begin{aligned} F_i(t) &= \Im\{(\overline{z_i(t) - z_0})(z_{i+1}(t) - z_0)\}, \quad i = 1, \ldots, n-1, \\ F_n(t) &= \Im\{(\overline{z_n(t) - z_0})(z_1(t) - z_0)\}. \end{aligned}$$

By the definition of a counterclockwise star formation and Lemma 2, $r_i(0) > 0$ and $0 < \alpha_i(0) < \pi$, where α_i, $i = 1, 2, \ldots, n$ are as in Figure 6. Hence, by Lemma 1, $F_i(0) > 0$, $\forall i$. We want to show that $F_i(t) > 0$ for all t, implying $r_i(t) > 0$ and $0 < \alpha_i(t) < \pi$ for all t, by Lemma 1. This means the points remain in a counterclockwise star formation.

Suppose by way of contradiction that some F_i, namely F_m, becomes zero at the first time t_1. We can select m such that $F_{m+1}(t_1) > 0$, for if all F_i's are zero at t_1, the points are all collinear,

by Lemma 1, which is a contradiction, by Lemma 3. Furthermore, for simplicity we renumber the indices if necessary so that $m+2 \leq n$. We have

$$\begin{aligned} F_m(t_1) &= 0 \\ F_{m+1}(t_1) &> 0 \\ F_i(t) &> 0 \qquad \forall t \in [0, t_1), \qquad i = 1, 2, \ldots, n\,. \end{aligned}$$

Taking the derivative along trajectories of the system $\dot{z} = Az$ and noting that $\dot{z}_0 = 0$ by Theorem 1, we have

$$\begin{aligned} \dot{F}_m &= \Im\{\overline{\dot{z}_m}(z_{m+1} - z_0)\} + \Im\{\overline{(z_m - z_0)}\dot{z}_{m+1}\} \\ &= \Im\{\overline{(z_{m+1} - z_m)}(z_{m+1} - z_0)\} + \Im\{\overline{(z_m - z_0)}(z_{m+2} - z_{m+1})\} \\ &= -2F_m + G_m, \end{aligned}$$

where $G_m = \Im\{\overline{(z_m - z_0)}(z_{m+2} - z_0)\}$. Observe that

$$G_m = r_m r_{m+2} \sin(\alpha_m + \alpha_{m+1})\,.$$

By Lemma 1, $F_m(t_1) = 0$ implies that at t_1 either $r_m = 0$; $r_{m+1} = 0$; $\alpha_m = 0$ and $r_m, r_{m+1} > 0$; or $\alpha_m = \pi$ and $r_m, r_{m+1} > 0$. We cannot have $r_{m+1} = 0$ since $F_{m+1}(t_1) > 0$. Condition $\alpha_m = \pi$ and $r_m, r_{m+1} > 0$ is also impossible, since $\alpha_i(t_1) \geq 0$, $\forall i$, so all the points are either on the line formed by z_{m+1} and z_m, a contradiction, or they are on or to one side of it, implying the centroid is not on the line formed by z_{m+1} and z_m, also a contradiction. So consider the case that $\alpha_m = 0$ and $r_m, r_{m+1} > 0$ at t_1. Then

$$G_m(t_1) = \frac{r_m}{r_{m+1}} F_{m+1}(t_1)\,.$$

Hence $G_m(t_1) > 0$. By continuity of G_m, there exists $0 \leq t_0 < t_1$ such that $G_m(t) > 0$ for all $t \in [t_0, t_1]$. Also, by assumption, $F_m(t) > 0$ for $t \in [0, t_1)$. Hence,

$$\dot{F}_m = -2F_m + G_m > -2F_m\,, \qquad t \in [t_0, t_1)\,.$$

Therefore

$$F_m(t) > \exp(-2(t - t_0))F_m(t_0) > 0\,, \qquad t \in [t_0, t_1)\,.$$

By continuity of F_m, $F_m(t_1) > 0$, a contradiction.

Finally, consider the case that $r_m = 0$ at $t = t_1$. Suppose that by a rotation of the coordinate system, if necessary, $z_{m+1}(t_1) = -r$, where $r = r_{m+1}(t_1) > 0$. Also, to keep the notation simple, we renumber the points so that $m = n - 1$. We have $\dot{z}_m(t_1) = z_{m+1}(t_1) - z_m(t_1) = -r$. Let $k < m$ be such that $r_k(t_1) \neq 0$ and $r_j(t_1) = 0$ for $j = k+1, \ldots, m$. Such a k exists, for if $r_j(t_1) = 0$ for all $j \neq m+1$, then 0 is not the centroid, a contradiction. Now if $n = 3$, we must have $\Im\{z_k(t_1)\} = 0$; otherwise 0 is not the centroid. Then, the points are all collinear, a contradiction by

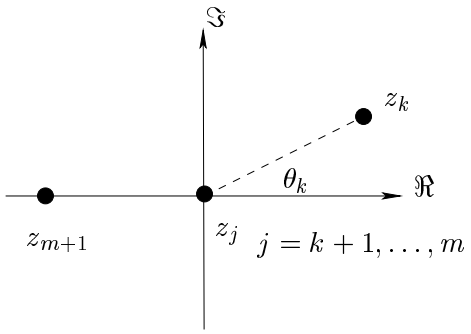

Figure 7: Illustration for points at t_1.

Lemma 3. If $n > 3$, since $\alpha_i(t_1) \geq 0$, $\forall i$, we must have that $\Im\{z_k(t_1)\} > 0$, for if $\Im\{z_k(t_1)\} = 0$ then $\Im\{z_i(t_1)\} \leq 0$, $\forall i$, implying the points are all collinear or the centroid is not 0, both contradictions. The geometry of the situation is depicted in Figure 7. Let $\theta_k(t_1) = \delta > 0$. By continuity of θ_k, there exists $t_0 < t_1$ such that for $t \in [t_0, t_1]$, $\theta_k(t) > \delta/2$. Since the points are in a counterclockwise star formation until t_1 we have that $\theta_m(t) > \theta_k(t)$ for $t \in [t_0, t_1)$. By definition

$$z_m(t_1) - z_m(t_1 - h) = h\dot{z}_m(t_1) + O(h)$$

where $O(h)/h \to 0$ as $h \to 0$. We obtain

$$\begin{aligned} \Re\{z_m(t_1 - h)\} &= rh + O(h) \\ \Im\{z_m(t_1 - h)\} &= O(h)\,. \end{aligned}$$

Thus, for $h > 0$ sufficiently small $\Re\{z_m(t_1 - h)\} > 0$ and we know $\Im\{z_m(t_1 - h)\} > \Re\{z_m(t_1 - h)\} \tan \delta/2$, with $0 < \delta/2 < \pi/2$. Combining these facts we obtain

$$O(h) > (rh + O(h)) \tan \delta/2\,.$$

Dividing by h and taking the limit as $h \to 0$ we obtain $\lim_{h\to 0} |O(h)/h| > r \tan \delta/2 > 0$, a contradiction. ■

3 A Strategy for Sensors with a Limited Field of View

In this section we study a different control strategy that is motivated by Reynolds' *cohesion* steering strategy, and provide a rigorous analysis by adopting some ideas in [3]. Suppose as before that there are n autonomous agents represented by points in the complex plane and numbered 1 through n; the agents don't need to know the labels. Each agent has a sensor with a limited field of view, in the sense that it can see and know the relative positions of only those agents that are within some distance of itself. And we call those neighbor agents. Let $N_i(t)$ denote the set of labels of agent i's neighbor agents at time t. Reynolds' *cohesion* strategy is for agent i to steer towards the *average*

of the neighbor agents' directions. For technical reasons (i.e., for a tractable stability problem), we consider where agent i steers towards the *sum* of the neighbor agents' directions. Thus the kinematic equation is

$$\dot{z}_i(t) = \sum_{j \in N_i(t)} [z_j(t) - z_i(t)], \quad i = 1, \ldots, n. \tag{6}$$

We use an undirected graph $\mathcal{G}$ with vertex set $\{z_1, z_2, \ldots, z_n\}$ to describe the sensor relationship among agents at time t: (z_i, z_j) is an edge just in case agents z_i and z_j are within sensor range of each other (all the sensors are assumed to have the same range). We call this the *sensor graph*. The sensor relationship changes over time, so the sensor graph changes too. Let $\{\mathcal{G}_p : p \in \mathcal{P}\}$ denote the class of all possible undirected graphs defined on n vertices. Corresponding to each graph $\mathcal{G}_p$, let $J_p \in \mathbb{R}^{n \times n}$ denote the adjacency matrix, whose ijth entry is 1 if (i, j) is an edge and 0 if not, let $D_p \in \mathbb{R}^{n \times n}$ denote the diagonal matrix whose ith diagonal element is the valence of vertex i, and define

$$A_p = J_p - D_p.$$

As an example, Figure 8 shows two sensor graphs for four agents. The two corresponding matrices are

$$A = \begin{bmatrix} -1 & 1 & 0 & 0 \\ 1 & -2 & 1 & 0 \\ 0 & 1 & -2 & 1 \\ 0 & 0 & 1 & -1 \end{bmatrix}, \quad A = \begin{bmatrix} -1 & 1 & 0 & 0 \\ 1 & -3 & 1 & 1 \\ 0 & 1 & -2 & 1 \\ 0 & 1 & 1 & -2 \end{bmatrix}.$$

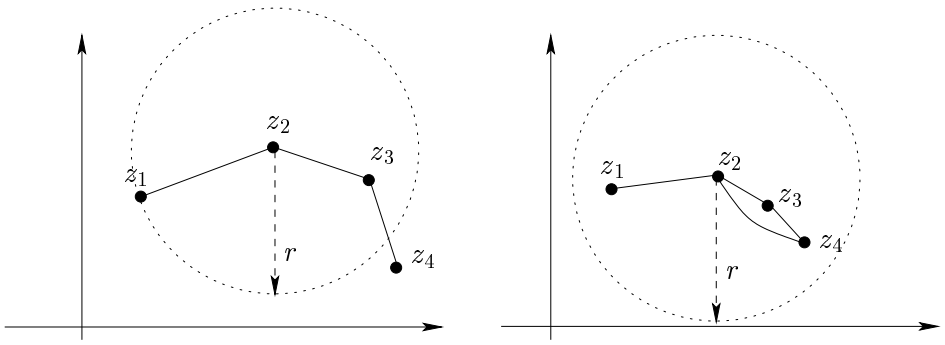

Figure 8: Two sensor graphs for four agents.

At time t, let the sensor graph be $\mathcal{G}_{p(t)}$ and let the corresponding matrix be $A_{p(t)}$. The overall system is then

$$\dot{z}(t) = A_{p(t)} z(t), \tag{7}$$

where $z(t)$ is the position vector. The signal $p(t)$ switches among a finite number of values as t progresses. It is *assumed* that chattering doesn't occur, that is, that $p(t)$ switches a finite number of times in every finite time interval. Then (7) has a well-defined solution.

Our goal is to show that, for a class of switching signals $p(t)$ and a class of initial configurations of the agents, all agents converge to the same point (i.e., the centroid). We need an assumption to prove this (the same assumption as in [3]), namely, that the sensor graph is always connected.

Theorem 4 *With regard to system (7), assume $\mathcal{G}_{p(t)}$ is connected for every $t \geq 0$. Then the centroid of the points $z_1(t), \ldots, z_n(t)$ is stationary and every $z_i(t)$, $i = 1, 2, \ldots, n$ converges to this centroid.*

The proof requires a lemma.

Lemma 4 *Let $A \in \mathbb{R}^{n \times n}$ be a real symmetrical matrix with eigenvalues λ_i satisfying $\lambda_n \leq \lambda_{n-1} \leq \cdots \leq \lambda_2 < \lambda_1 = 0$. Let $\mathcal{E}_0$ denote the eigenspace for $\lambda_1 = 0$ and let $\mathcal{E}_1$ denote the orthogonal complement of $\mathcal{E}_0$. Then for every $x \in \mathcal{E}_1$,*

$$x^T A x \leq \lambda_2 x^T x.$$

Proof Let $v_1, v_2, \ldots, v_n$ be normalized eigenvectors of A corresponding to the eigenvalues $\lambda_1 = 0, \lambda_2, \ldots, \lambda_n$. Then

$$A = \lambda_2 v_2 v_2^T + \cdots + \lambda_n v_n v_n^T.$$

So for $x \in \mathcal{E}_1$,

$$\begin{aligned} x^T A x &= \lambda_2 x^T v_2 v_2^T x + \cdots + \lambda_n x^T v_n v_n^T x \\ &\leq \lambda_2 (x^T v_2 v_2^T x + \cdots + x^T v_n v_n^T x) \\ &= \lambda_2 x^T (v_2 v_2^T + \cdots + v_n v_n^T) x \\ &= \lambda_2 x^T (v_1 v_1^T + v_2 v_2^T + \cdots + v_n v_n^T) x \\ &= \lambda_2 x^T x. \end{aligned}$$

■

Proof of Theorem 4: If $\mathcal{G}_p$ is connected, A_p has the properties that every row sum is equal to 0, the diagonal elements are less than 0, and the other elements are non-negative. Thus, letting a_{ij} denote the ijth element of A_p, we have

$$-a_{ii} = \sum_{j \neq i} a_{ij} > 0, \quad \forall i = 1, \ldots, n.$$

Hence, from Gerschgorin's theorem [18], we can conclude that the eigenvalues of A_p are in the set $\{\lambda : \text{Re } \lambda < 0 \text{ or } \lambda = 0\}$. In particular, the nonzero eigenvalues have negative real parts.

Next we observe, again when $\mathcal{G}_p$ is connected, that A_p has a unique zero eigenvalue, i.e., rank $A_p = n - 1$. To see this, note that D_p is nonsingular and define a new matrix

$$\tilde{A}_p = D_p^{-1} A_p = B_p - I, \quad B_p := D_p^{-1} J_p.$$

The associated graph $\mathcal{G}(J_p)$ is connected, and so is the associated graph $\mathcal{G}(B_p)$. Therefore, B_p is irreducible. By the Perron-Frobenius theorem [1], B_p has a unique largest real eigenvalue λ_1, and the other eigenvalues λ_i, $i = 2, \ldots, n$, satisfy Re $\lambda_i < \lambda_1$. So $\tilde{A}_p$, with eigenvalues $\{\lambda_1 - 1, \ldots, \lambda_n - 1\}$, has a unique largest real one. Using Gerschgorin's theorem again, we know that the eigenvalues of $\tilde{A}_p$ are in the set $\{\lambda : \text{Re } \lambda < 0 \text{ or } \lambda = 0\}$ and also we know that $\tilde{A}_p$ has a zero eigenvalue. Consequently, $\tilde{A}_p$ has a unique largest eigenvalue $\lambda_{max} = 0$, i.e., rank A_p = rank $\tilde{A}_p = n - 1$.

Now we proceed as in the proof of Theorem 1. For every t, $A_{p(t)}$ has $\lambda = 0$ as an eigenvalue of multiplicity 1 and the vector v of 1's is a common eigenvector. Thus $\mathcal{E}_0 = \text{span } \{v\}$ is a common eigenspace and its orthogonal complement, $\mathcal{E}_1$, is the sum of all the other eigenspaces, for all t. As before, the trajectory looks like

$$z(t) = av + w(t), \quad w(t) \in \mathcal{E}_1$$

and it remains to show that $w(t) \to 0$.

Since $w(t) = z(t) - av$ and $A_{p(t)}v = 0$,

$$\dot{w}(t) = \dot{z}(t) = A_{p(t)}z(t) = A_{p(t)}w(t).$$

We know that for any $w(0) \in \mathcal{E}_1$, the solution $w(t) \in \mathcal{E}_1$, $\forall t \geq 0$. In other words, $\mathcal{E}_1$ is a positively invariant set for the system $\dot{w}(t) = A_{p(t)}w(t)$. Choose the Lyapunov function

$$V(w) = \frac{1}{2}w^T w.$$

Take the derivative of $V(w(t))$ along the solution of $\dot{w}(t) = A_{p(t)}w(t)$:

$$\dot{V}(w(t)) = w^T(t)A_{p(t)}w(t).$$

¿From Lemma 4,

$$\dot{V}(w(t)) = w^T(t)A_{p(t)}w(t) \leq -W(w(t)),$$

where $W(w) := -(\max_p \lambda_{p1})w^T w$, λ_{p1} is the largest nonzero eigenvalue of A_p, and the max is over all p for which the sensor graph is connected. Thus

$$W(w) > 0, \quad \forall w \in \mathcal{E}_1 - \{0\}, \qquad \text{and} \qquad W(0) = 0.$$

Therefore, by the Lyapunov stability theorem for non-autonomous systems [8], the trajectory starting in $\mathcal{E}_1$ converges to 0. ■

We simulate twenty mobile autonomous agents using the local control strategy for sensors with a limited field of view. The initial locations of the twenty agents are generated randomly as shown in Figure 9. To understand the general effect of the size of the sensor range on the performance of asymptotical convergence to a single point, we carry out the simulation three times with the same initial positions as shown in Figure 9, but different sensor ranges. Specifically, for sensor range $r = 30, 25, 50$, the trajectories of the twenty agents are given in Figures 10, 11, and 12, respectively. The simulation results show that the sensor range $r = 25$ cannot guarantee that the sensor graph is connected all the time, and thus the agents do not converge to a single point but rather to two points. For the sensor ranges $r = 30, 50$, the sensor graph is always connected, and convergence to a single point results.

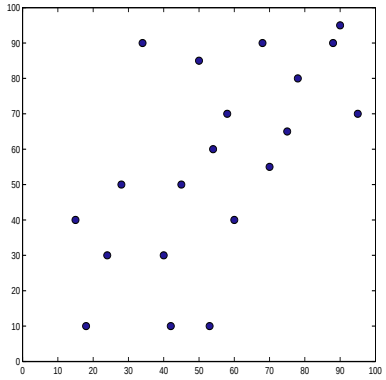

Figure 9: Initial locations.

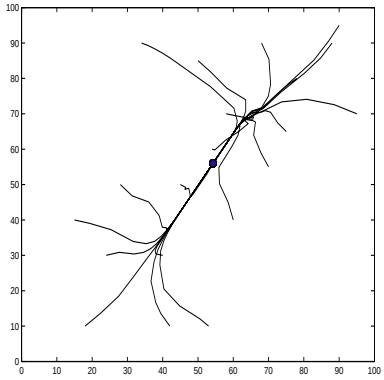

Figure 10: Trajectories (sensor range is 30).

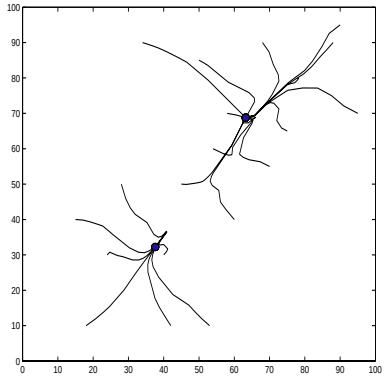

Figure 11: Trajectories (sensor range is 25).

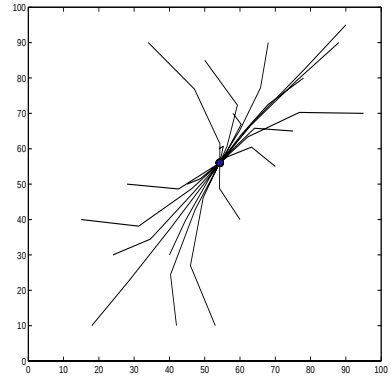

Figure 12: Trajectories (sensor range is 50).

4 A Strategy Based on a Linear Combination of the Subgroup

In the previous section, we considered where each autonomous agent can see and know only those agents within the disk of pre-specified radius about itself. Given the same radius, mutual visibility among the autonomous agents can naturally be represented by an undirected graph called a sensor graph. And under the assumption that the sensor graph is always connected, a group of mobile autonomous agents achieves a single point of convergence. Our next question is this: Is it possible to attain the same result or further results for any type of sensors with different constraints? For instance, the camera doesn't have a disk-like visibility but a cone-like field of view. In this section, we will present a general result that indicates the convergence of groups of agents to a single point for whatever field of view.

Suppose as before that there are n autonomous agents represented by points in the complex plane and numbered 1 through n; the agents don't need to know the labels. Let $N_i(t)$ denote the set of labels of those agents sensed by agent i at time t and let $n_i(t)$ denote the cardinality of $N_i(t)$ (the number of agents sensed by agent i at time t). We consider the local control strategy where each agent pursues the centroid of the subgroup of sensed agents at time t. In other words, each agent senses the positions of the subgroup of agents relative to itself and updates its velocity linearly by the sensed information. Thus, the kinematic equation is

$$\dot{z}_i(t) = \begin{cases} \frac{1}{n_i(t)} \sum\limits_{j \in N_i(t)} \{z_j(t) - z_i(t)\}, & n_i(t) \neq 0, \\ \qquad\qquad\qquad\qquad\qquad\qquad & i = 1, 2, \ldots, n. \\ 0, & n_i(t) = 0, \end{cases} \tag{8}$$

Now, we use a directed graph $\mathcal{G}$ with vertex set $\{z_1, z_2, \ldots, z_n\}$ to describe the sensor relationships among the group of agents at time t. The graph $\mathcal{G}$ is defined such that the directed edge from vertex i to vertex j is one of the graph's edges just in case agent i can sense agent j. And we still call this a sensor graph. Since the sensor relationships change over time, we use all such possible graphs to describe them. Let $\{\mathcal{G}_p : p \in \mathcal{P}\}$ denote a suitably defined set, indexing the class of all possible directed graphs $\mathcal{G}_p$ defined on n vertices. Corresponding to each directed graph $\mathcal{G}_p$, let $J_p \in \mathbb{R}^{n \times n}$ denote the adjacency matrix of the directed graph $\mathcal{G}_p$ on n vertices whose ijth entry is 1 if there is a directed edge from i to j, and 0 if there isn't, let $D_p \in \mathbb{R}^{n \times n}$ denote the diagonal matrix whose ith diagonal element is the number of directed edges from vertex i to others within the graph $\mathcal{G}_p$, and let $U_p \in \mathbb{R}^{n \times n}$ denote the diagonal matrix whose ith diagonal element is the reciprocal of the ith diagonal element of matrix D_p if it is not zero, and 0 if it is zero. And then we define

$$A_p = U_p(J_p - D_p), \qquad \forall p \in \mathcal{P}.$$

Thus, for example, two sensor graphs for four agents are shown in Figure 13. The two corresponding matrices are

$$A = \begin{bmatrix} -1 & 1 & 0 & 0 \\ 0 & 0 & 0 & 0 \\ 0 & 1 & -1 & 0 \\ 0 & 0 & 1 & -1 \end{bmatrix}, \qquad A = \begin{bmatrix} -1 & 1 & 0 & 0 \\ \frac{1}{2} & -1 & 0 & \frac{1}{2} \\ 0 & 1 & -1 & 0 \\ 0 & 0 & 1 & -1 \end{bmatrix}.$$

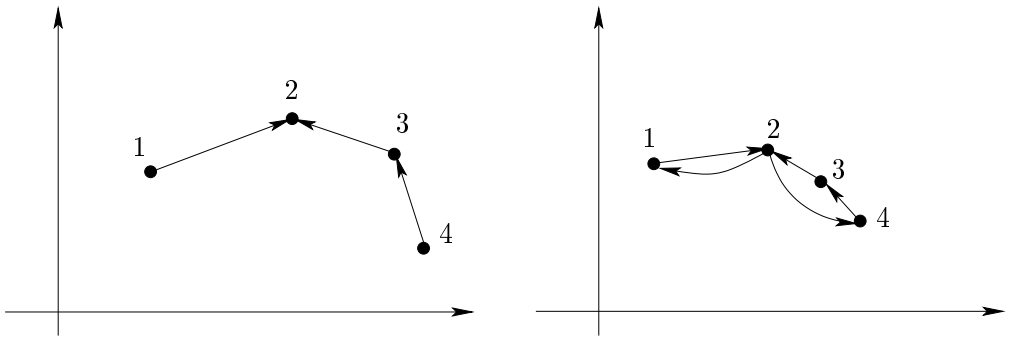

Figure 13: Two directed sensor graphs for four agents.

At time t, let the sensor graph be $\mathcal{G}_{p(t)}$ and let the corresponding matrix be $A_{p(t)}$. Then the overall system is

$$\dot{z}(t) = A_{p(t)} z(t), \tag{9}$$

where $z(t)$ is the position vector $z(t) = [\ z_1(t) \quad z_2(t) \quad \cdots \quad z_n(t)\ ]^T$, and $p(t) : \mathbb{R}^+ \longrightarrow \mathcal{P}$ is a piecewise constant switching signal whose value at time t is the index of the directed graph representing the sensor relationship at time t.

Our goal here is to show for a large class of switching signals $p(t)$ and for any initial positions of the agents that all the agents will converge to the same place in the plane. Obviously, if some agent never senses other agents, convergence cannot occur. Mathematically this would mean that the directed graph $\mathcal{G}_{p(t)}$ is never a connected graph. To avoid this situation, we could assume the directed graph is connected all the time. However, this assumption is too strong and we cannot guarantee it. So the situation of perhaps the greatest interest is that where $\mathcal{G}_{p(t)}$ might be disconnected only for some time and connected for some other time. We denote by $\mathcal{Q}$ the subset of $\mathcal{P}$ consisting of the indices of the strongly connected graphs in $\{\mathcal{G}_p : p \in \mathcal{P}\}$; strongly connected means that there exists at least one directed path from any vertex to any other vertex.

Theorem 5 *Let $z(0)$ be an initial position and let $p : \mathbb{R}^+ \longrightarrow \mathcal{P}$ be a piecewise constant switching signal for which there exists a positive T so that $p(t) \in \mathcal{Q}$ at least once in each time interval of length T. Then each $z_i(t)$ converges to the same point a, where a is a complex number depending only on $z(0)$ and $p(t)$.*

The following theorems about row stochastic matrices and a lemma about the diameter of a convex hull are central to the proof of Theorem 5. A square real matrix is *row stochastic* if it is nonnegative and its row sums all equal 1. (A *nonnegative matrix* is a one whose entries are all nonnegative.)

Theorem 6 [6] *Let $Q \in \mathbb{R}^{n\times n}$ and $P(t) = \mathrm{e}^{Qt}$. Then for every $t > 0$, $P(t)$ is row stochastic iff*

$$(a)\ Q_{ii} \le 0,\ \forall i; \quad (b)\ Q_{ij} \ge 0,\ \forall i \ne j; \quad (c)\ \sum_j Q_{ij} = 0, \quad \forall i.$$

For a matrix $P = (p_{ij}) \in \mathbb{R}^{n\times n}$, we define $\delta(P)$ by

$$\delta(P) := \max_j \max_{i_1,i_2} |p_{i_1 j} - p_{i_2 j}|.$$

Thus $\delta(P)$ measures how different the rows of P are. The rows of P are identical iff $\delta(P) = 0$. Also, we define $\lambda(P)$ by

$$\lambda(P) := 1 - \min_{i_1,i_2} \sum_j \min(p_{i_1 j}, p_{i_2 j}).$$

Then we have the following theorem.

Theorem 7 [11] *Let $\{P_1, P_2, \dots\}$ be a finite or infinite set of row stochastic matrices satisfying $0 \le \lambda(P_i) \le \beta < 1$. Then for each infinite sequence, $P_{k_1}, P_{k_2}, \dots$, there exists a row vector c such that*

$$\lim_{j\to\infty} P_{k_j} P_{k_{j-1}} \cdots P_{k_1} = \mathbf{1}c,$$

where $\mathbf{1} := [\ 1 \quad 1 \quad \cdots \quad 1\ ]^T$.

The version of Theorem 7 stated above is somewhat modified from the original version. The proof of the modified one is given as below.

Proof Since $0 \leq \lambda(P_i) \leq \beta < 1,\ i = 1, 2, \ldots,$

$$\lim_{j\to\infty} \prod_{m=1}^{j} \lambda(P_{k_m}) = 0.$$

Applying Lemma 2 in [11], $\delta(P_{k_j} P_{k_{j-1}} \cdots P_{k_1}) \leq \prod_{m=1}^{j} \lambda(P_{k_m})$, so

$$\lim_{j\to\infty} \delta(P_{k_j} P_{k_{j-1}} \cdots P_{k_1}) = 0.$$

Let $M_1 = P_{k_1},\ M_2 = P_{k_2}P_{k_1},\ \ldots,\ M_j = P_{k_j}P_{k_{j-1}} \cdots P_{k_1},\ \ldots,$ and specifically, let C_1^j be the first column of the matrix M_j and let c_m^j be the mth element of C_1^j. Then

$$\lim_{j\to\infty} \max_{m,n} |c_m^j - c_n^j| = 0.$$

Also, we know $C_1^j = P_{k_j} C_1^{j-1}$, that is, each element of C_1^j is a convex combination of elements of C_1^{j-1}, so

$$0 < \max_m(c_m^j) \leq \max_m(c_m^{j-1}) \quad \text{and} \quad 1 \geq \min_m(c_m^j) \geq \min_m(c_m^{j-1}),$$

and therefore, $\max_m(c_m^j)$ and $\min_m(c_m^j)$ converge as j approaches ∞, say $\lim_{j\to\infty} \max_m(c_m^j) = \alpha_1$ and $\lim_{j\to\infty} \min_m(c_m^j) = \beta_1$. Then we have

$$\lim_{j\to\infty} |\max_m(c_m^j) - \min_m(c_m^j)| = |\alpha_1 - \beta_1| = 0,$$

since $|\max_m(c_m^j) - \min_m(c_m^j)| = \max_{m,n} |c_m^j - c_n^j|$. Hence, $\alpha_1 = \beta_1$. Furthermore, notice that

$$\min_m(c_m^j) \leq c_m^j \leq \max_m(c_m^j),\ \forall\, m$$

so

$$\lim_{j\to\infty} c_m^j = \alpha_1.$$

That means

$$\lim_{j\to\infty} C_1^j = \mathbf{1}\alpha_1$$

and similarly for other columns of the matrix M_j. Therefore

$$\lim_{j\to\infty} P_{k_j} P_{k_{j-1}} \cdots P_{k_1} = \mathbf{1}c.$$

■

Lemma 5 *Let $V = \{v_1, v_2, \ldots, v_n\}$ be a finite set of points in $\mathbb{C}$ and let $P = Conv\{V\}$ be the convex hull of the set V. Then the diameter of the convex hull $d(P) := \max_{p_i, p_j \in P} \|p_i - p_j\|$ satisfies*

$$d(P) = \max_{v_r, v_s \in V} \|v_r - v_s\|.$$

Proof First we claim that p_1, p_2 are vertices of the convex hull P if $\|p_1 - p_2\| = d(P)$. To see this,

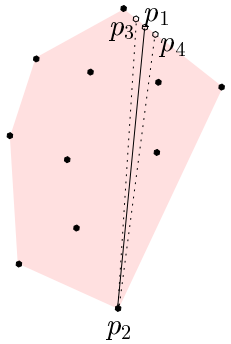

Figure 14: Illustration for the proof of Lemma 5.

suppose not. That is, at least one of p_1, p_2, say p_1, is in the interior of the convex hull or in one of the edges of P. If p_1 is in the interior of the convex hull, then we can find a point p_1' on the line p_1p_2 and still in P such that $\|p_1 - p_2\| < \|p_1' - p_2\|$. This contradicts that $\|p_1 - p_2\|$ is maximum. And if p_1 is in one of the edges of P, we can choose two points p_3, p_4 in this edge along different directions from point p_1 (see Figure 14). Then from trigonometry, the line segment $\overline{p_1p_2}$ is shorter than one of the line segments $\overline{p_3p_2}$, $\overline{p_4p_2}$, which contradicts that $\|p_1 - p_2\|$ is maximum.

On the other hand, suppose p' is a vertex of P. Then $Conv(V \backslash \{p'\})$ is not the same as the set $P = Conv(V)$, and so p' must be in the set V. As a result, the set of vertices of the convex hull is a subset of V. Also, $V \subset P$, we have

$$\max_{v_r, v_s \in V} \|v_r - v_s\| = \|p_1 - p_2\|,$$

from which the result follows. ■

Proof of Theorem 5: Suppose p changes its value at time instants $t_0 = 0 < t_1 < t_2 < \cdots$. If there are actually only finitely many switches, the final at t_m, artificially define $t_{m+j} = t_m + jb, j = 1, 2, \ldots$, where b is a finite positive value. So the time $\mathbb{R}^+$ can be divided into an infinite number of time intervals

$$[t_0, t_1), [t_1, t_2), \ldots, [t_i, t_{i+1}), \ldots.$$

Since $p(t)$ is piecewise constant, there exist $t_{max}, t_{min} > 0$ such that $t_{min} \leq t_{i+1} - t_i \leq t_{max}$. Also, $A_{p(t)} = A_{p(t_i)}, \ \forall t \in [t_i, t_{i+1})$.

The solution of system (9) is

$$z(t) = \mathrm{e}^{A_{p(t_i)}(t-t_i)}\mathrm{e}^{A_{p(t_{i-1})}(t_i-t_{i-1})}\cdots\mathrm{e}^{A_{p(t_0)}(t_1-t_0)}z(0).$$

We write the transition matrix

$$\Phi(t,t_i) = \mathrm{e}^{A_{p(t_i)}(t-t_i)}, \qquad i=0,1,2,\ldots, \quad t\in[t_i,t_{i+1}],$$

so

$$z(t) = \Phi(t,t_i)\Phi(t_i,t_{i-1})\cdots\Phi(t_1,t_0)z(0), \quad t\in[t_i,t_{i+1}].$$

For the given T, generate a subsequence $\{t_{m_j}\}$ of $\{t_i\}$ as follows: (1) Set $t_{m_0}=t_0=0$. (2) If $T\in(t_{i-1},t_i]$, set $t_{m_1}=t_i$. (3) If $t_{m_1}+T\in(t_{i-1},t_i]$, set $t_{m_2}=t_i$. And so on. Then taking $T_j=t_{m_j}$, we have

$$z(T_1) = \Phi(t_{m_1},t_{m_1-1})\Phi(t_{m_1-1},t_{m_1-2})\cdots\Phi(t_1,t_0)z(0) =: \Psi_1 z(0),$$

$$z(T_2) = \Phi(t_{m_2},t_{m_2-1})\Phi(t_{m_2-1},t_{m_2-2})\cdots\Phi(t_{m_1+1},t_{m_1})z(T_1) =: \Psi_2 z(T_1) = \Psi_2\Psi_1 z(0),$$

and so on so that

$$z(T_j) = \Psi_j\Psi_{j-1}\cdots\Psi_1 z(0).$$

First, we will show $\lim_{j\to\infty} z(T_j) = a\mathbf{1}$. It suffices to show that

$$\lim_{j\to\infty}\Psi_j\Psi_{j-1}\cdots\Psi_1 = \mathbf{1}c,$$

where c is a row vector. (Then $a=cz(0)$.)

The matrix A_p, $p\in\mathcal{P}$, satisfies (a) $A_{p_{ii}}\le 0$, $\forall i$; (b) $A_{p_{ij}}\ge 0$, $\forall i\ne j$; (c) $\sum_j A_{p_{ij}} = 0$, $\forall i$. Hence by Theorem 6, we know $\Phi(t_{i+1},t_i) = \mathrm{e}^{A_{p(t_i)}(t_{i+1}-t_i)}$ is row stochastic and the diagonal elements are lower-bounded by a positive value ϵ_1 since $\mathcal{P}$ is a finite set and $t_{i+1}-t_i$ is in the close interval $[t_{min},\ t_{max}]$.

Furthermore, for $p\in\mathcal{Q}$ (i.e., the graph $\mathcal{G}_p$ is strongly connected), $A_p = U_p(J_p-D_p) = U_pJ_p - I$, and the matrix $V_p := U_pJ_p$ is irreducible (i.e., for every (i,j) there exists a natural number q such that $v_{p_{ij}}^{(q)}>0$, where $v_{p_{ij}}^{(q)}$ denotes the (i,j) element of V_p^q). Hence,

$$\begin{aligned}\Phi(t_{i+1},t_i) &= \mathrm{e}^{A_{p(t_i)}(t_{i+1}-t_i)} = \mathrm{e}^{-I(t_{i+1}-t_i)}\mathrm{e}^{V_{p(t_i)}(t_{i+1}-t_i)}\\ &= \mathrm{e}^{-(t_{i+1}-t_i)}\left\{I + V_{p(t_i)}(t_{i+1}-t_i) + \frac{\left[V_{p(t_i)}(t_{i+1}-t_i)\right]^2}{2!}+\cdots\right\}.\end{aligned}$$

¿From the above expression, we can see that if $p\in\mathcal{Q}$, each element of $\Phi(t_{i+1},t_i)$ is lower-bounded by a positive value ϵ_2. That is, $\Phi(t_{i+1},t_i)\ge\epsilon_2 M$, $i=0,1,2,\ldots$, where M is a matrix with all elements 1, and the notation $\Phi(t_{i+1},t_i)\ge\epsilon_2 M$ means that $\Phi(t_{i+1},t_i)-\epsilon_2 M$ is nonnegative.

If $p(t) \in \mathcal{Q}$ happens at least once in each time interval of length T, then at least one of the transition matrices Φ in the matrix product

$$\Psi_j = \Phi(t_{m_j}, t_{m_j-1})\Phi(t_{m_j-1}, t_{m_j-2}) \cdots \Phi(t_{m_{j-1}+1}, t_{m_{j-1}}),\ j = 1, 2, \ldots.$$

is row stochastic with each element greater than ϵ_2, and the others are row stochastic matrices with each diagonal element greater than ϵ_1. In each time interval of length T, there are a finite number of switching times. Let's say the maximum number of switching times is K for every time interval of length T. As a result, $\Psi_j,\ j = 1, 2, \ldots$ is row stochastic and each element is lower-bounded by $\epsilon_2\epsilon_1^{K-1}$. Thus, $0 \leq \lambda(\Psi_j) \leq 1 - n\epsilon_2\epsilon_1^{K-1} < 1,\ j = 1, 2, \ldots.$

Therefore, by Theorem 7,

$$\lim_{j\to\infty} \Psi_j\Psi_{j-1} \cdots \Psi_1 = \mathbf{1}c,$$

where c is a row vector. That is,

$$\lim_{j\to\infty} z(T_j) = \mathbf{1}cz(0) = a\mathbf{1}.$$

Now we have to look at the times between the instants $\{0, T_1, T_2, \ldots\}$. We will show that

$$\max_{i_1,i_2} \|z_{i_1}(t) - z_{i_2}(t)\| \leq \max_{q_1,q_2} \|z_{q_1}(T_j) - z_{q_2}(T_j)\|, \qquad \forall\, t \in [T_j,\, T_{j+1}], \tag{10}$$

where $z_{i_1}(t)$, $z_{i_2}(t)$ are the elements of vector $z(t)$. For $t \in [T_j,\, T_{j+1}]$,

$$z(t) = \Phi(t, t_{m_j+k})\Phi(t_{m_j+k}, t_{m_j+k-1}) \cdots \Phi(t_{m_j+1}, t_{m_j})z(T_j) =: \widetilde{\Phi}z(T_j),$$

where $\widetilde{\Phi}$ is a row stochastic matrix since $\Phi(t, t_{m_j+k})$, $\Phi(t_{m_j+k}, t_{m_j+k-1})$, $\ldots$, $\Phi(t_{m_j+1}, t_{m_j})$ are all row stochastic matrices. Hence, $z_i(t)$, $i = 1, 2, \ldots, n$ is in the convex hull of the set $\{z_i(T_j),\ i = 1, 2, \ldots, n\}$. Then (10) follows from Lemma 5.

Therefore, we conclude that

$$\lim_{t\to\infty} z(t) = a\mathbf{1},$$

where a is a complex number depending only on $z(0)$ and $p(t)$. ■

Figure 15 shows a simulation for five autonomous agents to congregate at a common place using the local control strategy discussed in this section. Each agent has a cone-like field of view with infinite radius and 90 degree angle. The agent rotates its view angle 90 degree clockwise if there are no other agents in its field of view. From Figure 15, we can see that the initial sensor graph is not strongly connected. As the system evolves, the sensor graph might be strongly connected for some time and then disconnected for some other time.

Actually, it's not necessary for each agent to pursue the centroid of the subgroup of sensed agents to achieve a single point convergence. Considering a more general control strategy based on a linear combination of the subgroup, we have the general kinematic equation

$$\dot{z}_i(t) = \sum_{j\in N_i(t)} a_{ij}(t)[z_j(t) - z_i(t)], \qquad a_{ij} > 0, \quad i = 1, 2, \ldots, n, \tag{11}$$

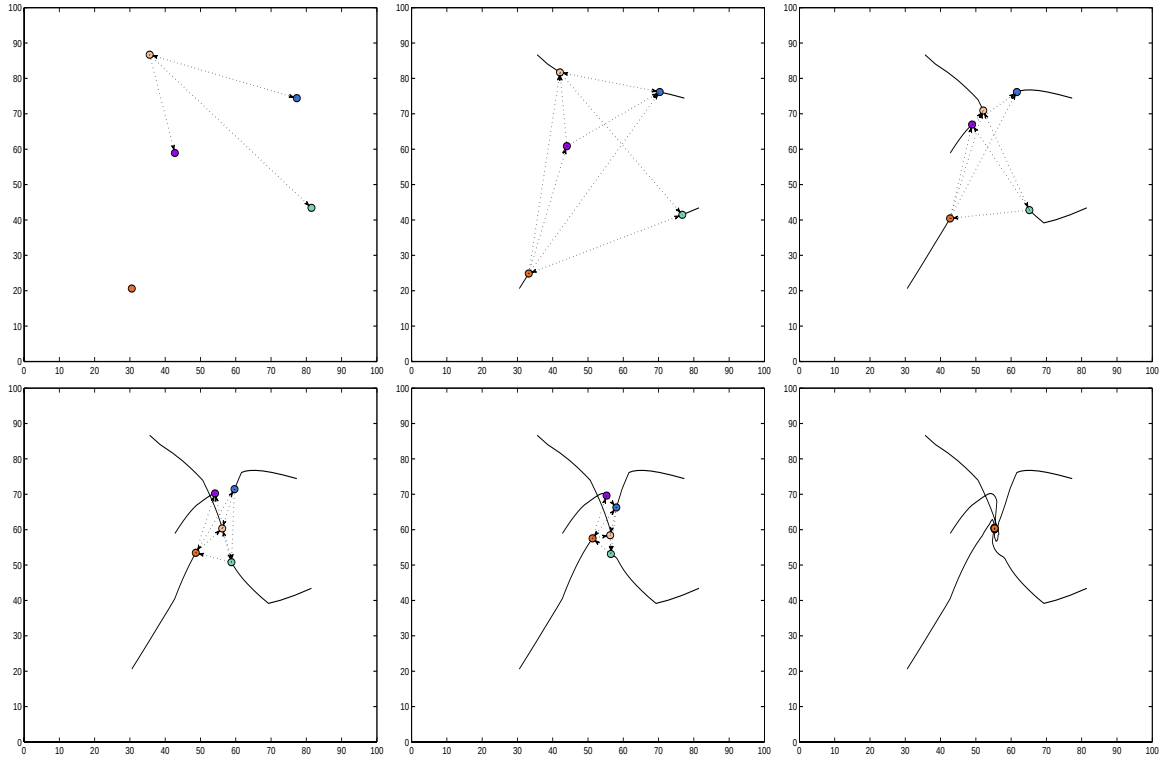

Figure 15: Trajectories of five agents and the sensor graphs as the system evolves.

or in vector form

$$\dot{z}(t) = \widetilde{A}(t)z(t), \tag{12}$$

where the diagonal elements of $\widetilde{A}(t)$ are $\widetilde{A}_{ii}(t) = -\sum_{j \in N_i(t)} a_{ij}(t)$ and the non-diagonal elements are $\widetilde{A}_{ij}(t) = \begin{cases} a_{ij}(t), & j \in N_i(t), \\ 0, & j \notin N_i(t). \end{cases}$

In the present context, system (8) can be viewed as a special case of (11) with $a_{ij}(t) = \frac{1}{n_i(t)}$, $\forall\, j \in N_i(t)$. However, the matrix $\widetilde{A}(t)$ has the same structural properties as the matrix $A_{p(t)}$ in system (9), so Theorem 5 applies directly.

To summarize, both the strategy based on sequential pursuit discussed in Section 2 and the strategy for sensors with a limited field of view discussed in Section 3 also can be viewed as special cases of this general control strategy. The former is the simplified version with $a_{ij}(t) = 1$, and $N_i(t) = i + 1,\ i = 1, 2, \ldots, n-1,\ N_n(t) = 1$. The latter is the simplified version with $a_{ij}(t) = 1$ and $N_i(t)$ containing the labels of agent i's neighbor agents at time t.

We conclude by briefly discussing the feasibility of implementing our control strategies using only local sensors. To be specific, let's focus on the control strategy

$$\dot{z}_1 = z_2 - z_1, \tag{13}$$

i.e., "agent 1 pursues agent 2." What generic sensing is required for such a strategy? With reference to Figure 16, let Σ_g denote the coordinate frame for the plane ("g" is for global). Agent 1 is assumed to have on it a fixed local coordinate system, Σ_1. It is assumed that as z_1 moves Σ_1 does not rotate with respect to Σ_g. Also, agent 1 is assumed to have a sensor that can measure the position with respect to Σ_1 of agent 2. Coordinate frame Σ_{g1} is the translation of Σ_1 to the origin of Σ_g. A complex number z represents a point in Σ_g; then ${}^1z$ denotes its representation in Σ_1; and likewise for ${}^{g1}z$. Thus ${}^1z_2$ is a complex number representing the position of agent 2 in agent 1's local coordinate system.

We have

$${}^1z_2 = {}^{g1}z_2 - {}^{g1}z_1.$$

Also, if there is an angle of rotation θ from Σ_{g1} to Σ_g, then

$${}^{g1}z_2 \mathrm{e}^{j\theta} = z_2$$

and similarly for z_1. Thus

$$z_2 - z_1 = {}^{g1}z_2 \mathrm{e}^{j\theta} - {}^{g1}z_1 \mathrm{e}^{j\theta} = {}^1z_2 \mathrm{e}^{j\theta}.$$

Also,

$${}^{g1}\dot{z}_1 = {}^{g1}\dot{z}_1 \mathrm{e}^{j\theta}.$$

Substituting the last two equations into (13) and cancelling $\mathrm{e}^{j\theta}$, we get

$${}^{g1}\dot{z}_1 = {}^1z_2. \tag{14}$$

The conclusion is that (13) and (14) are equivalent. Strategy (14) can be implemented with a local sensor on-board agent 1, and the assumption for equivalence is that Σ_1 doesn't rotate with respect to Σ_g.

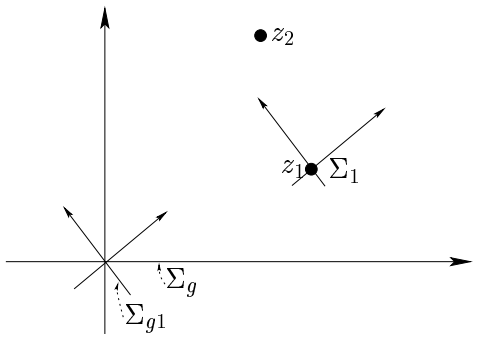

Figure 16: Global coordinate frame and local coordinate frame.

5 Conclusion

Control of systems consisting of multiple autonomous agents that are intended to perform a coordinated task is currently an important and challenging field of research. This is due to the broad range of applications of multi-agent systems in space missions, operations in hazardous environments, and military operations.

In this paper, we proposed three alignment strategies for coordinated control of groups of mobile autonomous agents modeled as point masses with full actuation. Each agent relies only on locally available information, namely, the relative locations of the sensed subgroup of agents. Global information and communication are not required. Instead, local sensors (perhaps vision) can be utilized to generate effective global behavior in groups of mobile autonomous agents. It was shown that the task of achieving a specified formation among a group of autonomous agents can be realized by our control strategies despite the absence of centralized coordination and despite the fact that the subgroup of the agents sensed by each agent changes over time as the system evolves. Also, we proved that three alignment strategies lead, under some assumptions, to the result that all agents converge to a single place.

Our future work includes developing our local control strategies for groups of mobile autonomous agents with more detailed vehicle dynamics or non-holonomic constraints, as well as the coupling of this work with the orientation control strategy.

References

[1] A. Berman and R.J. Plemmons, *Nonnegative Matrices in the Mathematical Sciences*, Academic Press, 1979.

[2] A. Bernhart, "Polygons of pursuit," *Scripta Mathematica*, 1956, pp. 23-50.

[3] A. Jadbabaie, J. Lin, and A.S. Morse, "Coordination of groups of mobile autonomous agents using nearest neighbor rules," *Proceedings IEEE Conference on Decision and Control*, 2002.

[4] C. Reynolds, "Flocks, birds, and schools: a distributed behavioral model," *Computer Graphics*, vol. 21, 1987, pp. 25-34.

[5] C. Reynolds, www.red3d.com/cwr/boids/

[6] D. Freedman, *Markov Chains*, Springer-Verlag, 1983.

[7] H. Ando, I. Suzuki, and M. Yamashita, "Formation and agreement problems for synchronous mobile robots with limited visibility," *Proceedings IEEE International Symposium on Intelligent Control*, 1995, pp. 453-460.

[8] H.K. Khalil, *Nonlinear Systems*, Prentice Hall, 1996.

[9] I. Suzuki and M. Yamashita, "Distributed anonymous mobile robots: formation of geometric patterns," *SIAM J. Comput.*, vol. 28, no. 4, 1999, pp. 1347-1363.

[10] J. Fredslund and M. J. Mataric, "A general algorithm for robot formation using local sensing and minimal communication," submitted to *IEEE Trans. on Robotics and Automation, Special Issue on Multi-Robot Systems*, 2001.

[11] J. Wolfowitz, "Products of indecomposable, aperiodic, stochastic matrices," *Proceedings American Mathematical Society*, vol. 14, no. 5, 1963, pp. 733-737.

[12] K. Sugihara and I. Suzuki, "Distributed motion coordination of multiple mobile robots," *Proceedings IEEE International Symposium on Intelligent Control*, 1990, pp. 138-143.

[13] N. E. Leonard and E. Fiorelli, "Virtual leaders, artificial potentials and coordinated control of groups," *Proceedings IEEE Conference on Decision and Control*, 2001, pp. 2968-2973.

[14] P. K. C. Wang, "Navigation strategies for multiple autonomous mobile robots moving in formation," *IEEE/RSJ International Workshop on Intelligent Robots and Systems*, 1989, pp. 486-493.

[15] P. K. C. Wang, "Navigation strategies for multiple autonomous mobile robots moving in formation," *Journal of Robotic Systems*, vol. 8, no. 2, 1991, pp. 177-195.

[16] Q. Chen and J. Y. S. Luh, "Coordination and control of a group of small mobile robots," *IEEE International Conference on Robotics and Automation*, 1994, pp. 2315-2320.

[17] R. Olfati-Saber and R.M. Murray, "Distributed cooperative control of multiple vehicle formations using structural potential functions," *IFAC World Congress*, 2002.

[18] R. Bhatia, *Matrix Analysis*, Springer-Verlag, 1996.

[19] Y. Oasa, I. Suzuki, and M. Yamashita, "A robot distributed convergence algorithm for autonomous mobile robots," *IEEE International Conference on Systems, Man, and Cybernetics*, 1997, pp. 287-292.

[20] Y. Oasa, I. Suzuki, and M. Yamashita, "Distributed memoryless point convergence algorithm for mobile robots with limited visibility," *IEEE Trans. on Robotics and Automation*, vol. 15, no. 5, 1999, pp. 818-828.